Colloids and Surfaces B: Biointerfaces 116 (2014) 211–218

Contents lists available at ScienceDirect

Colloids and Surfaces B: Biointerfaces

journal homepage: www.elsevier.com/locate/colsurfb

Preparation of graphene oxide-based surface plasmon resonance biosensor with Au bipyramid nanoparticles as sensitivity enhancer

Jia Zhang [a], Ying Sun [a], Qiong Wu [a], Yan Gao [a], Hua Zhang [a], Yu Bai [b], Daqian Song [a,*]

[a] College of Chemistry, Jilin University, Qianjin Street 2699, Changchun 130012, China
[b] Beijing National Laboratory for Molecular Sciences, College of Chemistry and Molecular Engineering, Peking University, Beijing 100871, China

ARTICLE INFO

Article history:
Received 9 August 2013
Received in revised form
12 December 2013
Accepted 2 January 2014
Available online 10 January 2014

Keywords:
Surface plasmon resonance
Graphene oxide
Au bipyramids, IgM

ABSTRACT

A sensitive and selective wavelength-modulation surface plasmon resonance (SPR) biosensor based on graphene oxide (GO) and Au bipyramids (AuBPs) is reported for determination of bovine IgM. GO sheets with lengths of 100–300 nm are synthesized and assembled on amine-modified Au film. The large surface area and abundant functional groups of GO allow the efficient immobilization of antibody. AuBPs are nanoparticles with a penta-twinned crystal structure, which have a sharp localized surface plasmon resonance (LSPR) band because of their high monodispersity. In the optimal conditions, the GO-based biosensor with AuBPs as sensitivity enhancers shows a satisfactory response to bovine IgM in the concentration range of 0.03–32 $\mu g\,mL^{-1}$. For contrast, traditional biosensor, GO-based biosensor and GO-based biosensor with Au nanorods (AuNRs) as sensitivity enhancers for antigen detection were also investigated. Consequently, the as-prepared GO sheets function as promising support for antibody and GO-based SPR biosensor using AuBPs as enhancers has the highest sensitivity among the four types of biosensors.

1. Introduction

Surface plasmon resonance (SPR) biosensors have become an indispensable tool for studying biomolecular interactions in pharmaceutical and biomedical research over the past decades. The number of reporting applications for analytes related to medical diagnostics, environmental monitoring, and food safety has been rapidly growing due to its label-free, high-sensitivity, real-time analysis and flexible system design [1]. One of the main drawbacks that impede further development of SPR applications is the lack of sufficient sensitivity to reliably detect small refractive index changes caused by compounds in low concentration at the sensing surface [2,3]. Some materials have been proposed to improve the performance of SPR biosensors, such as gold nanoparticles, magnetic nanoparticles, carbon nanotubes, electropolymerized molecularly imprinted polythiophenes [4–7].

Graphene, a 2D honeycomb lattice consisting of sp^2-hybridized carbons, has recently drawn much attention due to its distinct electronic, mechanical, optical and thermal properties from other carbon materials for various applications. A label-free, regenerative and sensitive surface plasmon resonance and electrochemical aptasensor based on graphene was first proposed for the detection of α-thrombin by Wang et al. [8]. The graphene sheets tend to form irreversible agglomerates and even restack to form graphite in solution because of the van der Waals interaction [9]. The oxidized counterpart of graphene, graphene oxide (GO), provides a new type of aqueous dispersible biocompatible material for biological applications [10]. Abundant oxygen-containing functional groups (carboxyl, epoxy, hydroxyl groups) and aromatic domains on its basal planes and edges enable GO to interact with varieties of biomolecules through covalent, noncovalent or electrostatic interactions [11–13]. GO-based sensors have been successfully applied to the detection of ss-DNA [14], metal ions [15], transferrin [12], Salmonella typhi and living cells [16,17]. Despite these demonstrations, it is highly desirable to develop more general schemes to expand the targets and enhance the performance for GO-based sensing.

Au nanoparticle is regarded as excellent material in immunoassay owing to its prominent optical property and facility of surface functionality. Au nanorods (AuNRs) show two plasmon resonance wavelengths defined as transverse and longitudinal mode, and the longitudinal plasmon wavelengths are more sensitive to the changes in the dielectric properties of the surroundings [18]. Therefore, AuNRs attracted tremendous attention and have been widely applied for the detection of various analytes. In addition, specially shaped, irregular gold nanoparticles have been demonstrated to be promising in clinical immunoassays and DNA hybridization analysis [19]. Au bipyramids (AuBPs) are nanoparticles with a penta-twinned crystal structure, which have a sharp and narrow localized surface plasmon resonance (LSPR) band because of their high monodispersity [20]. Nanoparticles with sharp tips (bipyramids, nanotriangles) exhibit especially high sensitivity to

* Corresponding author. Tel.: +86 431 85168399; fax: +86 431 85168399.
E-mail address: songdq@jlu.edu.cn (D. Song).

0927-7765/$ – see front matter © 2014 Elsevier B.V. All rights reserved.
http://dx.doi.org/10.1016/j.colsurfb.2014.01.003

the refractive index change of the surrounding medium as well as strong electromagnetic-field enhancement [21].

In this study, a novel GO-based SPR biosensor using AuBPs as sensitivity enhancers for the determination of bovine IgM is proposed. GO sheets are synthesized and assembled on the amine-modified SPR Au film via electrostatic interaction for antibody immobilization. When the antigen-AuBPs conjugates are selectively bound to the antibodies attached to the GO arrays, an obvious resonance wavelength shift of SPR biosensor could be observed. For contrast, traditional biosensor with MPA-modified SPR Au film, GO-based biosensor and GO-based biosensor with AuNRs as sensitivity enhancers for antigen detection were also investigated. The high loading capacity and good biocompatibility of GO together with remarkable optical property of AuBPs have been demonstrated to be beneficial to antibody immobilization and sensitivity enhancement of detection.

2. Materials and methods

2.1. Materials

Bovine IgM, rabbit anti-bovine IgM, human IgG, bovine IgG were purchased from Beijing Boisynthesis Biotechnology Company. Bovine serum albumin (BSA) was purchased from Ding Guo Biotechnology Company (Beijing, China). 3-Mercaptopropinic acid (MPA), 2-mercaptoethylamine (MEA), 1-ethyl-3-(3-dimethylaminopropyl)carbodiimide (EDC) and N-hydroxysuccinimide (NHS) were purchased from Jkchemical. Graphite was purchased from Sigma–Aldrich. Hydrogen tetrachloroauratehydrate ($HAuCl_4{\cdot}3H_2O$) was purchased from Acrosl. Silver nitrate, cethltrimethlammonium bromide (CTAB), hydrogen peroxide, sodium borohydride, sodium hydroxide, acetic acid, ethanol, and all other chemicals were of analytical reagent grade. All the solutions were prepared with ultra pure water, and all the glassware was cleaned with aqua regia before the experiments.

Bovine IgM, rabbit anti-bovine IgM, human IgG and bovine IgG were stored at −20 °C and all other biological reagents were stored at 4 °C. Sodium phosphate buffered saline (PBS, 0.01 mol L^{-1}, pH 7.4) was used as running buffer.

2.2. Equipment

The wavelength modulation SPR analyzer installed in our laboratory was used [22]. It is working with Kretschmann configuration to achieve the resonant condition by attenuated total reflection (ATR) in a prism (Fig. S1). A 2 nm adhesive layer of Cr followed by a 50 nm layer of Au was deposited on a K9 glass slide, then the glass slide with Au film was put on base of a prism (K9 glass) using a suitable index matching oil. A halogen tungsten lamp is used as the excitation light source. The light passes through a polarizer and two lenses and becomes TM-polarized parallel light. The parallel polychromatic light beam passes through the optical prism and excites surface plasmon at the interface between the Au film and the sample solution. The output light from another side of prism passes through the third optical focusing lens. One end of the optical fiber is put at the focal point of focusing lens and then the light beam has access to optical fiber as much as possible. The opposite end is connected to the spectrophotometer. Thus the output light is guided into the optical fiber and then enters the spectrophotometer (HR2000+, Ocean Optics Inc., USA). The HR2000+ spectrometer integrates a high-resolution optical bench, a powerful 2 MHz analog-to-digital (A/D) converter, programmable electronics, a 2048-element CCD-array detector and a high-speed USB 2.0 port. This combination produces extremely fast spectrometer and provides resolution to 0.035 nm (full width at half maximum, FWHM).

2.3. Procedures

2.3.1. Synthesis of GO

GO was prepared using a modification of Hummers and Offeman's method from graphite powders [23,24]. In a typical reaction, 0.5 g of graphite, 0.5 g of $NaNO_3$, and 23 mL of H_2SO_4 were stirred together in an ice bath. Next, 3 g of $KMnO_4$ was slowly added. Once mixed, the solution is transferred to a 35 °C water bath and stirred for about 1 h. Next, 40 mL of water was added, and the solution was stirred for 30 min while the temperature was raised to 90 °C. Finally, 100 mL of water was added, followed by the slow addition of 3 mL of H_2O_2 (30%). The warm solution was then filtered and washed with 100 mL of water. The filter cake was then dispersed in water by mechanical agitation. Low-speed centrifugation was done at 1000 rpm for 3 min. It was repeated until all visible particles were removed (about 3–5 times). The supernatant then underwent three more high-speed centrifugation steps at 8000 rpm for 30 min to remove small GO pieces and water-soluble byproduct.

2.3.2. Synthesis of antigen-AuBP conjugates and antigen-AuNR conjugates

AuBPs were chemically synthesized by a seed-mediated growth procedure with slight modifications [25]. Briefly, 20 mL of aqueous solution containing $HAuCl_4$ (0.125 mmol L^{-1}) and trisodium citrate (0.25 mmol L^{-1}) were added into an Erlenmeye flask. 0.3 mL of ice-cold $NaBH_4$ (10 mmol L^{-1}) solution was added into the solution under vigorous stirring for 2 min. The resulting gold seed solution appeared dark pink and should be kept for at least 2 h at room temperature. 1 mL of $HAuCl_4$ (10 mmol L^{-1}) and 20 mL of CTAB (100 mmol L^{-1}) were mixed in the presence of 0.2 mL of $AgNO_3$ (10 mmol L^{-1}). The resulting solution was referred to as the growth solution. Then, 0.4 mL of hydrochloric acid (1.0 mol L^{-1}) and 0.16 mL of ascorbic acid (100 mmol L^{-1}) were sequentially added into the growth solution. 180 μL of the seed solution was then added into the growth solution. The resulting solution was mixed by gentle inversion for 10 s and kept at 28 °C overnight. Finally, the solution was centrifuged at 12,000 rpm for 25 min twice to remove the excess CTAB, and the precipitate was suspended in 10 mL of water. EDC/NHS linking chemistry was used for the covalent attachment of antigen onto the surface of AuBPs. Prior to the analysis, 10 μL of 10 mg mL^{-1} BSA was added to each solution of antigen-AuBP conjugates to block the nonbinding sites of AuBPs. AuNRs were chemically synthesized by a seed-mediated growth procedure [26,27]. Biofunctionalized nanorod conjugates were prepared by the same EDC/NHS linking procedure.

2.3.3. Modification process to fabricate the SPR sensing surface

After PBS buffer was injected into the flow cell, 10 mmol L^{-1} MEA was injected into the flow cell and incubated for 1 h to form amine-modified Au film. Subsequently, 0.5 mg mL^{-1} GO was injected and assembled on the Au film via electrostatic interaction. Then the carboxyl groups of GO were activated with NHS (1.5 mmol L^{-1}) under the catalysis of EDC (7.5 mmol L^{-1}) for 25 min. PBS buffer was injected as the baseline solution. After the resonant wavelength kept constant, rabbit anti-bovine IgM were injected into the flow cell to covalently attach to the GO surfaces. After 12 h, PBS buffer was injected to wash off unbound antibody and stabilize the baseline. Prior to the analysis, 1 mol L^{-1} ethanolamine hydrochloride (pH 8.0) was used to block the non-specific binding sites.

2.3.4. Immunoassay

Antigen-AuBP conjugates at different concentrations were separately injected into the flow cell over the immobilized antibody

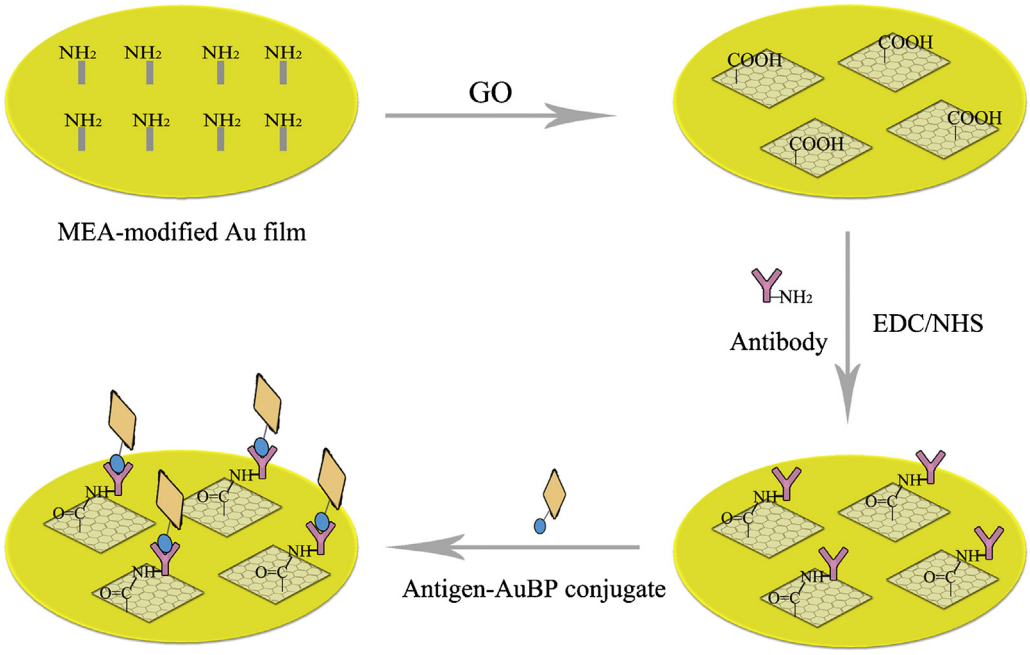

Fig. 1. A schematic diagram of experimental procedure. ( ) antibody, ( ) antigen, ( ) Au bipyramid, ( ) GO sheets.

surface. After the resonant wavelength kept constant, PBS was injected into the flow cell for 30 min. Due to a large amount of ions in the PBS, the antigen can be dissociated from the antibody immobilized on the surface of the biosensor and removed from the flow cell by impulse injection of the PBS [28]. When the antigen was dissociated from the antibody on the biosensor surface, another sample was injected into the flow cell. All experiments were conducted in triplicate to examine the reliability of the assays. A schematic of the fabricated biosensor is shown in Fig. 1.

To evaluate the selective binding of bovine IgM, bovine IgG and human IgG were determined by the same procedure as that used to detect bovine IgM.

3. Results and discussion

3.1. Synthesis and characterization of GO, AuNR and AuBP

Atomic force microscope (AFM) was used to confirm the formation of the single layer GO sheet. As shown in Fig. 2a, the thickness of GO sheet is about 0.943 nm, which is typical for single layered sheet of GO and similar to that reported previously [15]. The FTIR and UV–vis absorption spectra of GO further provide the information of the GO sheets (Fig. S2). The characteristic vibrations of GO are a broad and intense peak of O—H group at 3406 cm^{-1}, a C=O peak at 1731 cm^{-1}, a C—OH stretching peak at 1220 cm^{-1}, a C—O stretching peak at 1095 cm^{-1}, and a peak attributed to the vibration of graphitic skeletal domains and the adsorbed water molecules at 1620 cm^{-1}. These results indicate that the surface of GO was functionalized with different kinds of oxygen-containing functional groups. AuNRs of which the average length and width are about 50 nm and 20 nm were synthesized and characterized by transmission electron microscope (TEM) images and UV–vis absorption spectra in Fig. 2b. It is known that the absorption spectra of rod-shaped gold nanoparticles exhibited two plasmon absorption bands corresponding to the longitudinal band along the long axis (SP_{long}, at a longer wavelength depending on the aspect ratio of AuNRs) and the transverse band assignable to the short axis (SP_{trans}, at a shorter wavelength), respectively [29]. The UV–vis absorption spectra of prepared AuNRs show two absorbsion peaks at 646 nm and 520 nm (Fig. 2b). The AuBPs were synthesized by a seed-mediated growth procedure with slight modifications. Similar to AuNRs, AuBPs also have two surface plasmon resonance peaks corresponding to the electron oscillations along the longitudinal and transverse directions. The longitudinal surface plasmon (LSP) wavelength can be tuned systematically by varying the ratio of the height to the base-edge length [30]. The UV–vis absorption spectra of prepared bipyramids show two absorption peaks at 773 nm and 528 nm. The average length and width of the bipyramids are about 52 nm and 22 nm, respectively (Fig. 2c).

X-ray photoelectron spectroscopy (XPS) is a significant measure to observe the structure of C for carbon-based materials. XPS (KRATOS, AXIS ULTRA) measurements were carried out by using a monochromatized Al Kα (1486.7 eV) X-ray source. Fig. 3A shows the C 1s XPS spectra of GO. The C 1s spectra of GO could be deconvoluted into four peaks at 284.8, 286.8, 287.9, and 289.0 eV, which are associated with C—C, C—O, C=O, and O—C=O groups, respectively [31]. The crystalline structure of the synthesized samples was characterized by X-ray diffraction (XRD) using a diffractometer with Cu Kα radiation (Shimadzu Lab X XRD-6000). Figure 3B shows the XRD pattern of GO which has a peak centered at 2θ (scattering angles) = 11.4°, corresponding to the (0 0 2) inter-planar spacing around 7.75 Å. The most common peak around 26° for graphite is absent in GO sample. The result indicates the graphite has been well oxidized.

3.2. Preparation of sensing substrate based on GO sheets

For a GO-based SPR biosensor, 2-mercaptoethylamine (MEA) jointed strongly to the gold film surface by its sulfide bonds, and the amines terminal group lead to a positively charged Au film. The subsequent assembly of MEA and GO onto the Au film is investigated by the SPR technique. GO spontaneously assembles on the positively charged Au film due to electrostatic interaction between GO and MEA, resulting in a maximum shift of resonance wavelength of 7.20 nm. Taking consideration of the possible background increase, the in situ SPR curves before and after the GO assembly are shown in Fig. S3. The adsorption of sheets leads to the red shift of the SPR resonant wavelength and very limited background increase, yet almost no influence on the shape of SPR curve. The GO sheet consists of a hexagonal ring-based carbon network

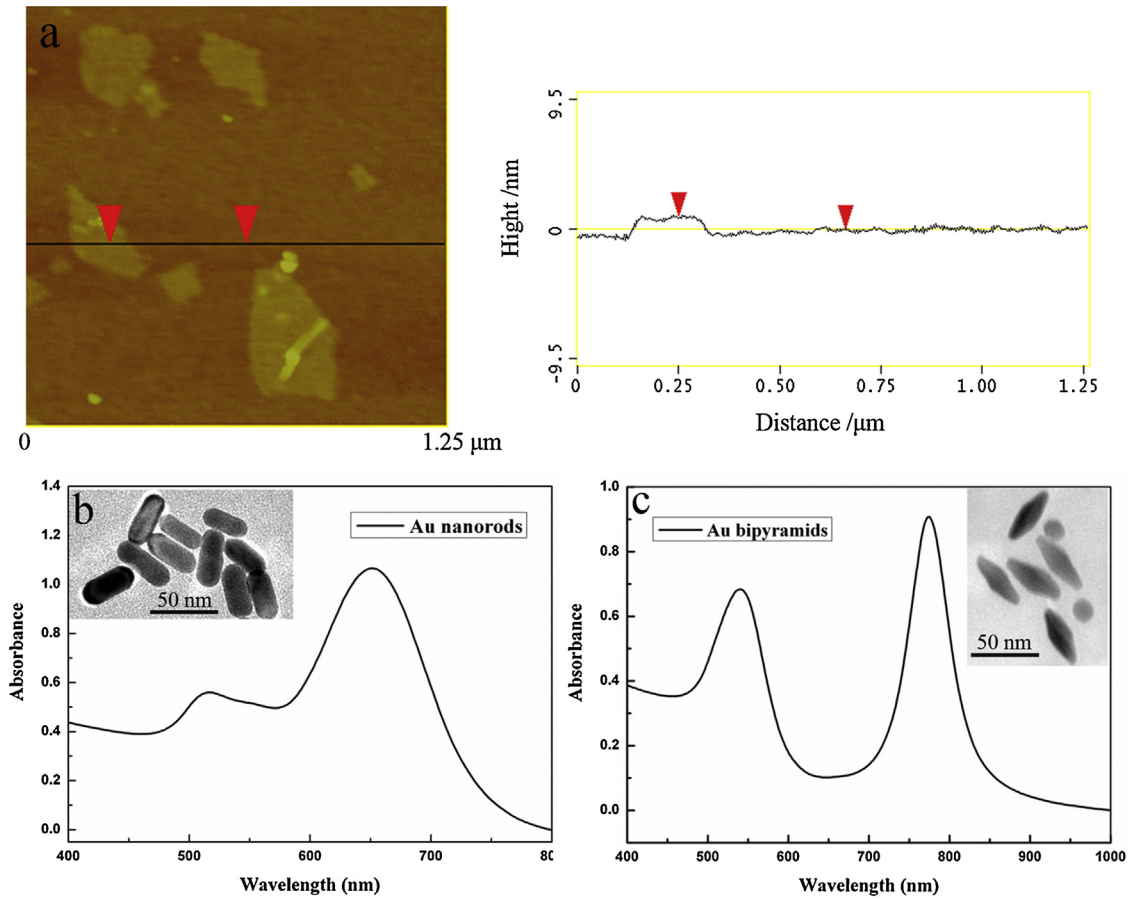

Fig. 2. Atomic force microscopy (AFM) image of GO (a) and UV–vis absorption spectra and TEM image of AuNRs (b) and AuBPs (c).

having both sp^2 -hybridized and sp^3 -hybridized carbons bearing hydroxyl and epoxide functional groups on either side of the sheet, whereas the sheet edges are mostly decorated by carboxyl and carbonyl groups. In the previous application, GO was used as matrix for enzyme immobilization [32]. The enzyme immobilization on the GO sheets could take place readily without using cross-linking reagents and additional surface modification and the maximum loading of enzyme is much higher than the loadings on many reported materials. Because of the large surface area and its interaction with the target biomolecules, this enrichment can be utilized to enhance the sensitivity of the biomolecules detection. After the GO sheets were assembled on amino-modified Au film, the carboxyl groups were further activated by EDC/NHS. This is a universal technique to conjugate carboxyl to amine groups in peptides and proteins. EDC reacts with a carboxylic acid to form an amine-reactive intermediate. Then, in the presence of NHS, the amine-reactive intermediate can be converted to amine-reactive NHS esters. As a result, rabbit anti-bovine IgM could be immobilized on the GO layers through covalent attachment between the amine groups of antibodies and the activated carboxyl groups of GO sheets [33]. The GO sheets decorated with antibody exhibit specific detection of antigen.

In order to select the optimum concentration of antibody, rabbit anti-bovine IgM at different concentrations were separately injected into the flow cell. The effect of the concentration of rabbit anti-transferrin on the shift of the resonant wavelength is shown in Fig. 4A. With the increase of the concentration, more antibodies were immobilized on the GO surface, resulting in the resonant wavelength moving to the longer wavelength. After the antibodies immobilized on the GO surface reached saturation, the resonant wavelength kept a constant value [22]. When the concentrations of rabbit anti-bovine IgM are 50, 75, 100 and 125 $\mu g\,mL^{-1}$, the shifts of resonant wavelength are 6.90, 11.00, 12.90 and 13.10 nm, respectively. Relatively high concentration of antibodies might result in stereo hindrance. Therefore, 100 $\mu g\,mL^{-1}$ was chosen as the optimum concentration for the detection of bovine IgM. The traditional substrate based on MPA-modified Au film was also investigated. Figure 4B shows the kinetic adsorption curves of 100 $\mu g\,mL^{-1}$ rabbit anti-bovine IgM obtained with the biosensor based on MPA-modified Au film (curve a) and GO-modified Au film (curve b). As shown in Fig. 4B, the maximum resonant wavelength shift for the immobilization of antibodies is 12.90 nm for GO-modified Au film and 7.2 nm for traditional MPA-modified Au film within 60 min. The situ SPR curves of antibody immobilization are given in Fig. S4. Obviously, the amount of rabbit anti-bovine IgM immobilized on GO surface is larger than that immobilized on MPA. The large surface area and high loading capacity for target biomolecules of GO are beneficial to the antibody immobilization. Meanwhile, the red shift of resonant wavelength in some wavelength range is beneficial to the sensitivity of wavelength-modulation SPR biosensor [34,35].

3.3. *Preparation of antigen-AuBP conjugates and antigen-AuNR conjugates*

The preparation of stable biofunctionalized AuBPs which interact specifically with their intended protein target is essential for improving SPR performance. EDC/NHS linking chemistry was used for the covalent attachment of antigens onto AuBPs. For the AuBPs-enhanced immunoassay, the ratio between antigens and AuBPs was optimized. The solution containing 8 μg bovine IgM and different concentrations of activated AuBPs was separately injected

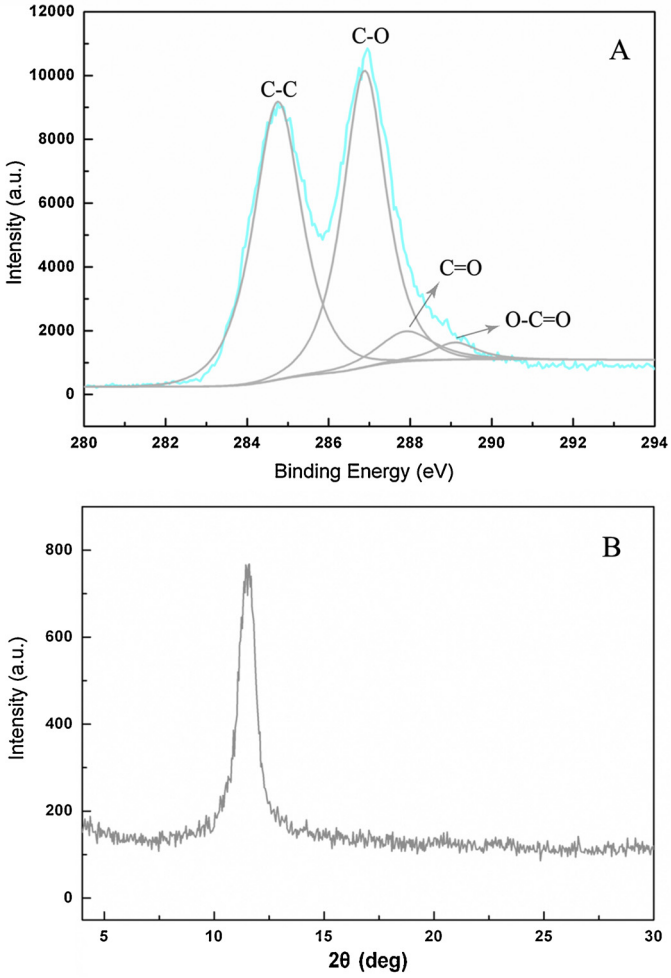

Fig. 3. The C 1s XPS spectra and XRD pattern of graphene oxide.

into the flow cell to evaluate the effect of the volume of activated AuBPs solution. The effect of the volume of activated AuBPs solution is shown in Fig. S5. The SPR response signal increases with the amount of activated AuBPs bound on the surface of the biosensor and then levels off. As a result, 0.12 ml as-prepared AuBPs solution was selected as the optimum volume to connect with 8 μg bovine IgM. It should be noted that 10 μL of 10 mg mL^{-1} BSA was added to each solution of antigen-AuBP conjugates to block the nonbinding sites of AuBPs and to avoid interaction between AuBPs and antibodies. In control experiment, 0.14 ml as-prepared AuNRs solution was selected as the optimum volume to connect with 8 μg bovine IgM.

3.4. Determination of antigen

In this report, traditional SPR biosensor, GO-based SPR biosensor, GO-based SPR biosensor with AuNRs as amplification labels, and GO-based SPR biosensor with AuBPs as amplification labels

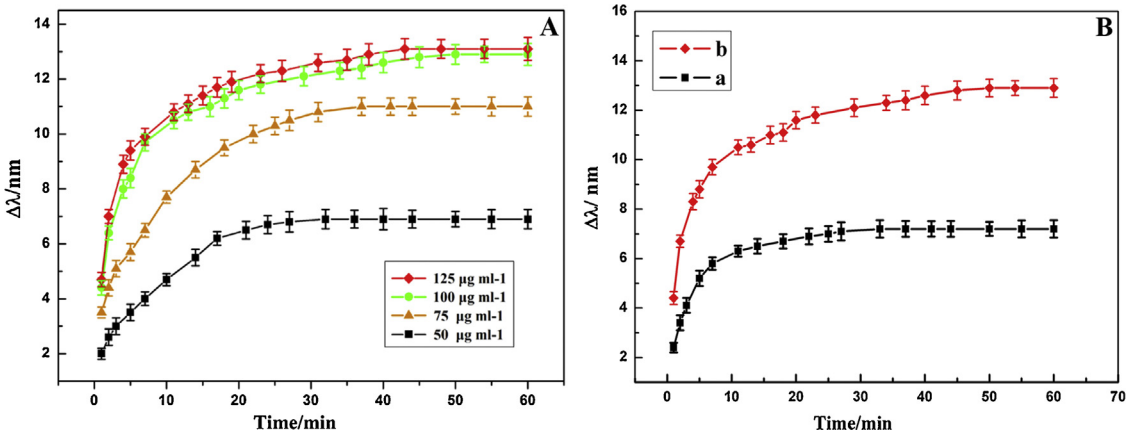

Fig. 4. (A) The kinetic adsorption curves of rabbit anti-bovine IgM on GO-modified Au film at different concentrations. (B) the kinetic adsorption curve of rabbit anti-bovine IgM at the concentration of 100 μg mL^{-1} on MPA-modified Au film (curve a) and GO-modified Au film (curve b). Error bar = ±S.D. and $n = 3$.

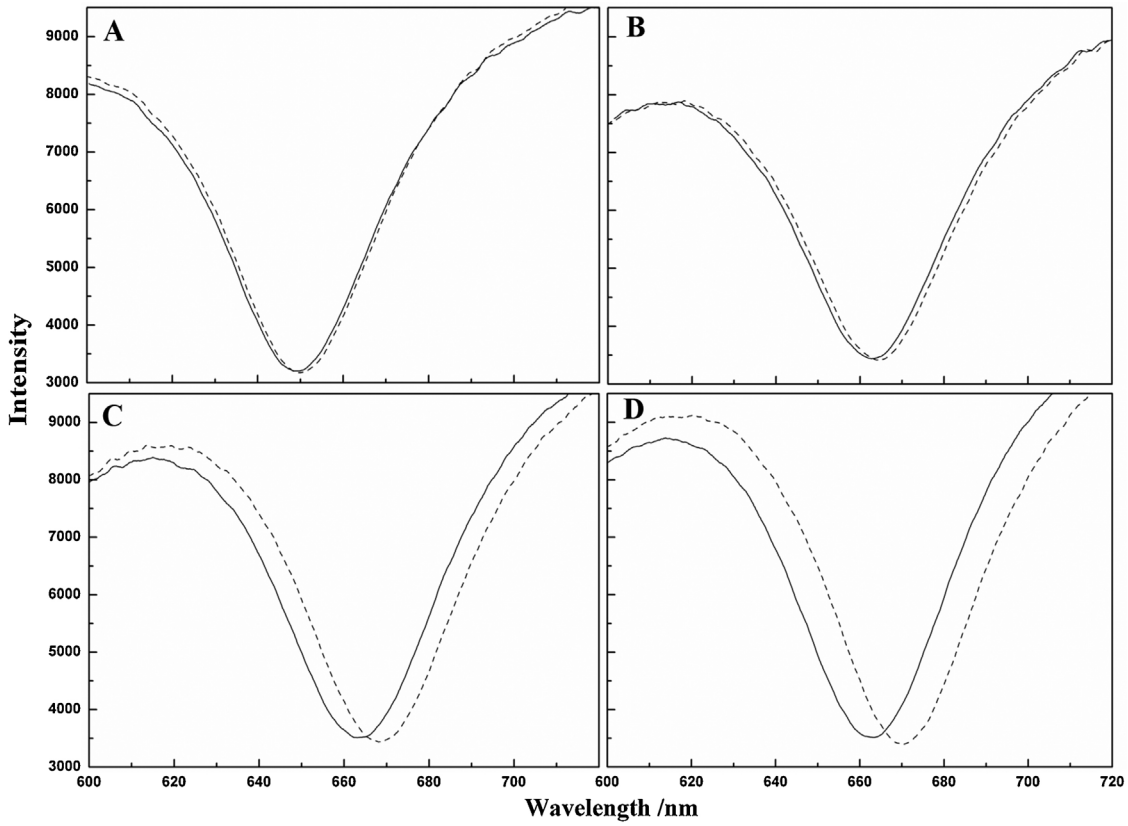

Fig. 5. In-situ SPR curves of detection of 4 μg mL^{-1} bovine IgM based on different systems. (A) MPA-modified Au film; (B) GO-modified Au film; (C) GO-modified Au film with antien-AuNR conjugates; (D) GO-modified Au film with antien-AuBP conjugates.

were constructed. To demonstrate the potential sensitivity of proposed SPR biosensor based on GO substrate and AuBPs, bovine IgM at different concentrations was separately injected into the flow cell at room temperature. The shifts of resonant wavelength due to antibody-antigen immunoreaction were measured. Fig. 5 shows the SPR spectrum for detection of 4 μg mL^{-1} bovine IgM in different methods. Under the same concentration of rabbit anti-bovine IgM, incubation of the Au-MPA-antibody substrate with 4 μg mL^{-1} solution of bovine IgM yields 1.0 nm shifts in resonant wavelength (Fig. 5A). While the exposure of Au-GO-antibody substrate to 4 μg mL^{-1} solution of bovine IgM results in 1.4 nm shift in resonant wavelength (Fig. 5B). When the antigen-AuNR and antigen-AuBP conjugates were used in GO-based biosensor, the shifts of resonant wavelength for 4 μg mL^{-1} solution of bovine IgM are 4.8 nm (Fig. 5C) and 7.0 nm (Fig. 5D), respectively. The significant increase in signal of the interaction between anti-bovine IgM and bovine IgM was afforded through the use of GO sheets as substrate and AuBPs as amplification labels.

Fig. 6 illustrates the variation of the resonant wavelength shifts as a function of different concentrations of bovine IgM in four types of biosensors. The SPR biosensor based on GO and antigen-AuBP conjugates shows a good response to bovine IgM in the concentration range of 0.03–32.00 μg mL^{-1}. The minimum shift of resonant wavelength is 0.20 nm at 0.03 μg mL^{-1} and the maximum shift is 17.20 nm at 32.00 μg mL^{-1}. The SPR biosensor based on GO and antigen-AuNR conjugates shows a good response to bovine IgM in the concentration range of 0.12-32.00 μg mL^{-1}. The shift of resonant wavelength is 0.20 nm at 0.12 μg mL^{-1} and 10.8 nm at 32.00 μg mL^{-1}. The SPR biosensor based on GO-modified Au film shows a response to bovine IgM in the concentration range of 0.5–32.00 μg mL^{-1}. The shift of resonant wavelength is 0.20 nm at 0.5 μg mL^{-1} and 3.8 nm at 32.00 μg mL^{-1}. The SPR biosensor based on traditional Au film shows a response to bovine IgM in the concentration range of 1.0–32.00 μg mL^{-1}. The shift of resonant wavelength is 0.20 nm at 1.0 μg mL^{-1} and 2.40 nm at 32.00 μg mL^{-1}. The limit of quantification (LOQ) is defined as the lowest measured concentration adjusted by three times of the standard deviation of the multiple measurements. The LOQ obtained with the biosensor based on GO and antigen-AuBP conju-

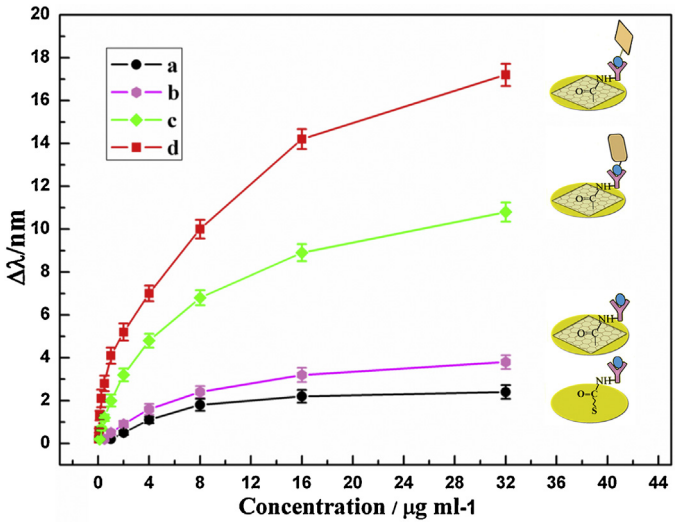

Fig. 6. The relationship between the shifts of the resonant wavelength and the different concentrations of bovine IgM: the biosensor based on MPA-modified Au film (a); the biosensor based on GO-modified Au film (b); the biosensor based on GO-modified Au film and antigen-AuNR conjugates (c); the biosensor based on GO-modified Au film and antigen-AuBP conjugates (d). Error bar = ±S.D. and n = 3.

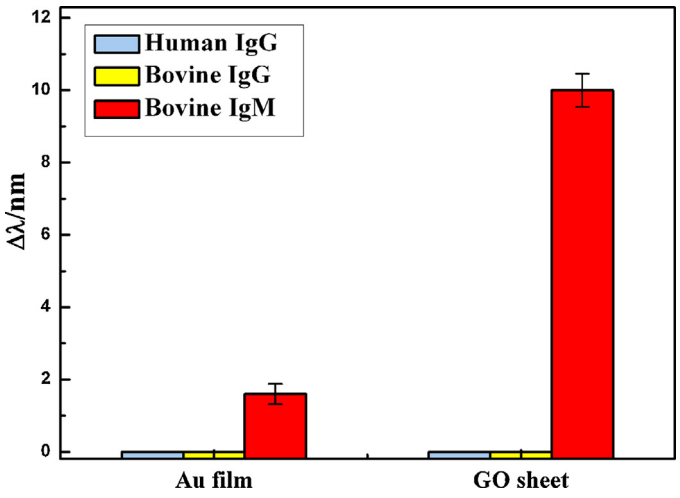

Fig. 7. The shifts of resonant wavelength measured obtained with different antigens based on different sensing membrane. Error bar = ±S.D. and $n = 3$.

gates is about 32 times lower than that obtained with traditional SPR biosensor, 16 times lower than that obtained with GO-based biosensor and 4 times lower than that obtained with the sensor based on GO and antigen-AuNR conjugates.

A GO-based detection platform has several advantages for optical sensing of biomolecules compared with conventional molecular beacons. The two-dimensional sheet is equipped with a range of functional groups that can interact in an ionic, covalent or non-covalent manner, so that in principle it provides the highest extraction efficiencies of biomolecules per unit area of virtually any material [36]. The high water solubility, large surface area and high loading capacity for target biomolecules of GO are beneficial to the antibody immobilization of SPR biosensor.

Differing from employing common spherical nanoparticles or nanorods, AuBPs were used to induce electromagnetic coupling and amplify the response of the binding of antigen to antibody. Under the same concentration of rabbit anti-bovine IgM, exposing the GO surface decorated with antibodies to antigen-AuBP conjugates yielded a dramatic enhancement of signal. The binding of antigen-AuBP conjugates with antibody immobilized on GO surface lead to large changes in the refractive index and obvious resonant wavelength shift. Compared with nanorods, bipyramid structures have sharper tips at their poles. Sharp features will present an additional advantage for molecular detection at the microscopic level in that a sharp tip creates a localized sensing/mode volume of highly enhanced electric field intensity [37], then SPR signal can be more significantly enhanced when AuBPs were used. On the other hand, the field magnitude is nonuniform for nanorods and bipyramids. The field magnitude decreases from the center toward the poles in the case of nanorods, but increases rapidly in the case of bipyramids [38]. Therefore, AuBPs exhibit especially high sensitivity to the refractive index change of the surrounding medium as well as strong electromagnetic-field enhancement, making AuBPs promising candidates for biosensing and plasmonic enhancement. In addition, the thickness of the sensing membrane increases and the resonant wavelength moves to longer wavelength, which also leads to the sensitivity enhancement of the wavelength-modulation SPR biosensor. The experiment results demonstrate that the use of GO as immobilization platform and AuBPs as amplification labels in SPR biosensor permitted 32 times enhancement in LOQ.

The specificity is also demonstrated by detecting human IgG and bovine IgG under the same conditions. After the rabbit anti-bovine IgM was immobilized on the activated surface of the biosensor, AuBPs-conjugated human IgG and AuBPs-conjugated bovine IgG at the concentrations of 8 $\mu g\,mL^{-1}$ were separately injected into the flow cell for 40 min (Fig. 7). There are no observable shifts of the resonant wavelength. The result confirms that the GO-based strategy using AuBPs as sensitivity enhancers has sufficient specificity and bovine IgM can be identified with high selectivity.

4. Conclusion

In summary, GO sheets possessing long-term stability, friendly biocompatibility and high loading capacity for target biomolecules serve as ideal platform for the antibody immobilization. AuBPs with a penta-twinned crystal structure have been proved to be promising sensitivity enhancers in biosensing. The GO-based SPR biosensor using AuBPs as sensitivity enhancers exhibits a satisfactory response in the concentration range of 0.03–32 $\mu g\,mL^{-1}$ for bovine IgM detection, which is more sensitive than traditional SPR biosensor, GO-based SPR biosensor and GO-based SPR biosensor using AuNRs as sensitivity enhancer.

Acknowledgments

This work was supported by National Natural Science Foundation of China (Nos. 20727003, 21075049, and 21105037), Program for New Century Excellent Talents in University (No. NECT-10-0443), Special-funded Programme on National Key Scientific Instruments and Equipment Development (No. 2012YQ090194) and Science and Technology Developing Foundation of Jilin Province (Nos. 20100356, and 20110162).

Appendix A. Supplementary data

Supplementary material related to this article can be found, in the online version, at doi:10.1016/j.colsurfb.2014.01.003

References

[1] J. Ladd, H.L. Lu, A.D. Taylor, V. Goodell, M.L. Disis, S.Y. Jiang, Colloids Surf. B 70 (2009) 1.
[2] J. Wang, Small 1 (2005) 1036.
[3] C.F. Gao, Z.D. Lu, Y. Liu, Q. Zhang, M.F. Chi, Q. Cheng, Y.D. Yin, Angew. Chem. Int. Ed. 51 (2012) 5629.
[4] L.A. Lyon, M.D. Musick, M.J. Natan, Anal. Chem. 70 (1998) 5177.
[5] J.L. Wang, A. Munir, Z.H. Li, H.S. Zhou, Biosens. Bioelectron. 30 (2009) 124.
[6] L.Y. Wang, Y. Sun, J. Wang, J. Wang, A.M. Yu, H.Q. Zhang, D.Q. Song, Colloids Surf. B 84 (2011) 484.
[7] R.B. Pernites, R.R. Ponnapati, R.C. Advincula, Macromolecules 43 (2010) 9724.
[8] L. Wang, C.Z. Zhu, L. Han, L.H. Jin, M. Zhou, S.J. Dong, Chem. Commun. 47 (2011) 7794.
[9] C. Xu, X. Wang, J.W. Zhu, J. Phys. Chem. C 112 (2008) 19841.
[10] M.R. Das, R.K. Sarma, R. Saikia, V.S. Kale, M.V. Shelke, P. Sengupta, Colloids Surf. B 83 (2011) 16.
[11] L.P. Cai, R.Y. Zhan, K.Y. Pu, X.Y. Qi, H. Zhang, W. Huang, B. Liu, Anal. Chem. 83 (2011) 7849.
[12] J. Zhang, Y. Sun, B. Xu, H. Zhang, Y. Gao, H.Q. Zhang, D.Q. Song, Biosens. Bioelectron. 45 (2013) 230.
[13] X.M. Sun, Z. Liu, K. Welsher, J.T. Robinson, A. Goodwin, S. Zaric, H.J. Dai, Nano Res. 1 (2008) 203.
[14] H.F. Dong, W.C. Gao, F. Yan, H.X. Ji, H.X. Ju, Anal. Chem. 82 (2010) 5511.
[15] Y.Q. Wen, F.F. Xing, S.J. He, S.P. Song, L.H. Wang, Y.T. Long, D. Li, C.H. Fan, Chem. Commun. 46 (2010) 2596.
[16] V.V. Singh, G. Gupta, A. Batra, A.K. Nigam, M. Boopathi, P.K. Gutch, B.K. Tripathi, A. Srivastava, M. Samuel, G.S. Agarwal, B. Singh, V. Rajagopalan, Adv. Funct. Mater. 22 (2012) 2352.
[17] Q.Y. He, H.G. Sudibya, Z.Y. Yin, S.X. Wu, H. Li, F. Boey, W. Huang, P. Chen, H. Zhang, ACS Nano 4 (2010) 3201.
[18] H.J. Parab, C. Jung, J.H. Lee, H.G. Park, Biosens. Bioelectron. 26 (2010) 667.
[19] Z.P. Wang, J.Q. Hu, Y. Jin, X. Yao, J.H. Li, Clin. Chem. 52 (2006) 1958.
[20] S. Lee, K.M. Mayer, J.H. Hafner, Anal. Chem. 81 (2009) 4450.
[21] M.J. Banholzer, N.J. Harris, E. Millstone, G.C. Schatz, C.A. Mirkin, J. Phys. Chem. C 114 (2010) 7521.
[22] J. Wang, L.Y. Wang, Y. Sun, X.N. Zhu, Y.B. Cao, X.H. Wang, H.Q. Zhang, D.Q. Song, Colloids Surf. B: Biointer. 75 (2010) 520.
[23] W.S. Hummers, R.E. Offeman, J. Am. Chem. Soc. 80 (1958) 1339.

[24] S. Gilje, S. Han, M. Wang, K.L. Wang, R.B. Kaner, Nano Lett. 7 (2007) 3394.
[25] K.M. Mayer, F. Hao, S. Lee, P. Nordlander, Nanotechnology 21 (2010) 255503.
[26] N.R. Jana, L. Gearheart, C.J. Murphy, Adv. Mater. 13 (2001) 1389.
[27] B. Nikoobakht, M.A. El-Sayed, Chem. Mater. 15 (2003) 1957.
[28] R. Pei, X. Cui, X. Yang, E. Wang, Talanta 53 (2000) 481.
[29] C.G. Wang, Y. Chen, T.T. Wang, Z.F. Ma, Z.M. Su, Chem. Mater 19 (2007) 5809.
[30] M.B. Mohamed, V. Volkov, S. Link, M.A. El-Sayed, Chem. Phys. Lett. 317 (2000) 517.
[31] Y.X. Xu, H. Bai, G.W. Lu, C. Li, G.Q. Shi, J. Am. Chem. Soc. 130 (2008) 5856.
[32] J.L. Zhang, F.H. Zhang, J.X. Yang, L. Huang, H. Liu, J.Y. Zhang, S.W. Guo, Langmuir 9 (2010) 6083.
[33] J.H. Jung, D.S. Cheon, F. Liu, K.B. Lee, T.S. Seo, Angew. Chem. Int. Ed. 49 (2010) 5708.
[34] J. Homola, Sens. Actuators B 41 (1997) 207.
[35] J. Homola, I. Koudela, S.S. Yee, Sens. Actuators B 54 (1999) 16.
[36] K.P. Loh, Q.L. Bao, G. Eda, M. Chhowalla, Nature Chem. 2 (2010) 1015.
[37] J. Homola, Chem. Rev. 108 (2008) 462.
[38] M.Z. Liu, P.C. Sionnest, T.W. Lee, S.K. Gray, Phys. Rev. B 76 (2007) 235428.